

Thermal stability simulations of 1,1-bis(*tert*-butylperoxy)-3,3,5-trimethylcyclohexane mixed with metal ions

An-Chi Huang¹ · Wei-Chun Chen¹ · Chung-Fu Huang¹ · Jing-Yu Zhao² · Jun Deng² · Chi-Min Shu¹

Received: 19 January 2017 / Accepted: 29 April 2017 / Published online: 8 May 2017
© Akadémiai Kiadó, Budapest, Hungary 2017

Abstract 1,1-Bis(*tert*-butylperoxy)-3,3,5 trimethylcyclohexane (TMCH), a typical organic peroxide, is normally an initiator agent and cross-linking agent of styrene and polyethylene. Metal ions, used as catalysis substances, can affect the thermal stability of TMCH. However, they are commonly found everywhere in processing areas such as in rusty rotating equipment, metal containers, and aging pipelines. Thus, we investigated the thermal stability of TMCH mixed with metal ions and acquired thermokinetic parameters using calorimetric data. Through isoconversional kinetic analysis simulations, thermokinetic parameters were obtained under isothermal conditions using nonisothermal experimental data. In DSC experiments, the E_a of TMCH mixed with CuCl_2 was lower than that of pure TMCH. TMR_{iso} of pure TMCH was shorter than that of TMCH mixed with CuCl_2 in isothermal experiments. The results of the simulations and experiments were compared and discovered to be similar. The results can be a reference for TMCH mixing with metal ions during its storage and transportation.

Keywords Organic peroxide · Metal ions · Thermokinetic parameters · Calorimetric data · Isoconversional kinetic analysis

List of symbols

A	Frequency factor (s^{-1})
E_a	Apparent activation energy (kJ mol^{-1})
k	Heat transfer coefficient ($\text{W m}^{-2} \text{K}$)
m	Mass (mg)
M	Number of metal atoms (dimensionless)
Q	Total stored energy (J)
R	Gas constant ($8.314 \text{ J mol}^{-1} \text{K}$)
t	Time (s)
T	Absolute temperature ($^{\circ}\text{C}$)
T_0	Apparent onset temperature ($^{\circ}\text{C}$)
T_{\max}	Maximum temperature ($^{\circ}\text{C}$)
TMR_{iso}	Isothermal time to maximum heating rate (h)
T_p	Peak temperature ($^{\circ}\text{C}$)
W	Molecular weight of compound (g mol^{-1})
X	Number of carbon atoms (dimensionless)
Y	Number of hydrogen atoms (dimensionless)
Z	Number of oxygen atoms (dimensionless)
ΔH_d	Heat of decomposition (J g^{-1})
α	Conversion degree (dimensionless)
β	Heating rate ($^{\circ}\text{C min}^{-1}$)

Introduction

Peroxides can be mainly divided into organic peroxides (OPs) and inorganic peroxides. Inorganic peroxides are generally oxidizing substances and are unreactive. By contrast, OPs are unstable and potentially explosive when exposed to thermal sources or even mechanical impact. Thus, the storage, transportation, manufacturing, and disposal of OPs can be dangerous. Under unexpected situations, OPs might cause accidents if the peroxy functional groups ($-\text{O}-\text{O}-$) in them decompose, because this produces

✉ Chi-Min Shu
shucm@yuntech.edu.tw

¹ Graduate School of Engineering Science and Technology, National Yunlin University of Science and Technology, 123, University Rd., Sec. 3, Douliou, Yunlin 64002, Taiwan, ROC

² School of Safety Science and Engineering, Xi'an University of Science and Technology, 58, Yanta Mid. Rd., Xi'an 710054, Shaanxi, People's Republic of China

an enormous amount of heat and pressure and engenders fires or explosions [1–8].

OPs are affected by their external environment, such as thermal sources or high temperatures, exposure to which may result in fire, explosion, toxic release, or other destruction that is detrimental to the environment [9] and additionally has costly social effects. The OP 1,1-bis(*t*-butylperoxy)-3,3,5-trimethylcyclohexane (TMCH) is used as a catalyst in polymerization reactions and as a cross-linking agent in the chemical industry. The CAS number of TMCH is 6731-36-8. Being intrinsically unstable and thermally reactive, this OP can trigger runaway reactions when mixed with acids, bases, or metal ions because the mixing process induces catalytic reactions [10–16]. Some metal ions adversely affect the thermal stability of TMCH. Metal ions are commonly present everywhere in manufacturing equipment such as rotating equipment, metal containers, and aging pipelines. Most storage containers, waste storage tanks, and pipelines are made of metal, such as copper or iron, which can age and rust, and using these for the storage and transport of TMCH may trigger a runaway reaction [17].

We investigated the thermal hazard characteristics and incompatible reactions of TMCH when it is mixed with various metal ion solutions, such as copper chloride (CuCl_2) and ferric chloride (FeCl_3), to determine how related thermal explosions could be prevented [18]. Thermokinetic parameters, including the apparent onset temperature (T_0), heat of decomposition (ΔH_d), and maximum temperature (T_{max}), were detected by differential scanning calorimetry (DSC) [19]. Through isoconversional kinetic analysis using nonisothermal experimental data, we obtained isothermal thermokinetic parameters including the isothermal time to maximum heating rate (TMR_{iso}), highest or peak heat flow, reaction time, and apparent activation energy (E_a) at different isothermal temperatures (60.0, 70.0, 80.0, and 90.0 °C). We conducted isothermal tests using thermal activity monitor III (TAM III) to identify the differences between the simulation and isothermal experimental results.

The results of this study can be used as a reference for the reactions caused by the mixing of TMCH and metals during the storage and transportation of TMCH. Inherently safer equipment could thus be designed for TMCH storage and transportation to avoid endangering the manufacturing system under adverse conditions [20–22].

Experimental

Sample preparations

To assess the reaction and determine the related thermokinetic parameters of TMCH when mixed with

metal ions (copper and iron), we purchased 88.0 mass% TMCH from ACE Chemical Corporation, Taiwan, and stored it in a refrigerator at 4.0 °C. The chemical structural formula of TMCH is illustrated in Fig. 1. TMCH was mixed with commonly used and commercially available metal ion solutions. CuCl_2 and FeCl_3 , diluted with distilled water to 5.0 mass%, were used in this study. The oxygen balance (OB %) of the organic peroxide and other compounds was calculated using [23–26]

$$\text{OB}\% = \frac{-1600}{W} \times \left(2X + \left(\frac{Y}{2} \right) + M - Z \right) \quad (1)$$

where W is the molecular weight of the compound (g mol^{-1}) and M , X , Y , and Z are the numbers of metal, carbon, hydrogen, and oxygen atoms, respectively. Moreover, the sample mass of each experiment is listed in Tables 2–8.

DSC

The DSC apparatus used contained reference and target samples, a furnace, and a thermal resistance material. The outer wall of the entire body of the furnace was wrapped in an adiabatic shell to prevent heat loss and external temperature interference. The DSC apparatus combined with STAR^c software was used to measure the heating of the chemical substances during a warming scan, and the material's endothermic and exothermic energy changes and basic thermal safety parameters were evaluated. The reference and target samples were heated in the same furnace simultaneously, leading to each sample having a different temperature and causing the target sample to release energy during thermal decomposition. Accordingly, the heat of decomposition in the cell was determined.

Programmable temperature control was used during the DSC tests, with various heating and cooling rates from 0.01 to 750.0 °C min^{-1} used and target sample temperatures from –150.0 to 700.0 °C detected. To ensure favorable equilibrium was attained during heating, we used heating rates β of 0.5, 1.0, 2.0, 4.0, and 8.0 °C min^{-1} , and the temperature range considered was 30.0–300.0 °C. Each set

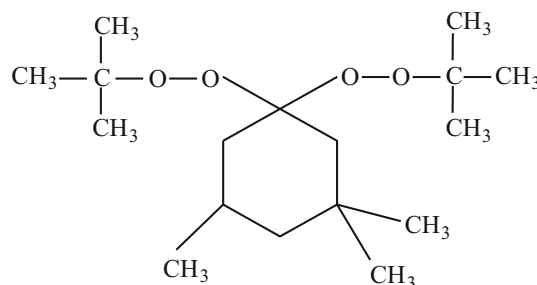


Fig. 1 Chemical structural formula of TMCH [1, 8]

of experiments was produced at least three times to ensure repeatability. The results of DSC were averaged to list the calorimetric data. The Kissinger formal model was applied to evaluate the kinetics. In addition, linear regression was employed to determine the apparent activation energy E_a from the regression slope. We obtained various heating rates and peak temperatures using DSC:

$$\frac{2.303[\log(\beta/T_{\max}^2)]}{1/T_{\max}} = \frac{-E_a}{R} \quad (2)$$

Thermal simulation using isoconversional kinetic analysis

Differential isoconversional kinetic analysis was used to estimate the thermal stability of the TMCH–metal ion mixtures under the temperature conditions employed. We imported DSC experimental data and calculated kinetic parameters, such as TMR_{iso} and E_a , to predict the response mode under isothermal and nonisothermal conditions [27–29]. The relationship between conversion rate and absolute temperature was used to determine E_a (α):

$$\frac{d\alpha}{dt} = A(\alpha) \exp\left[-\frac{E_a(\alpha)}{RT(t)}\right] f(\alpha) \quad (3)$$

$$A'(\alpha) = A(\alpha)f(\alpha) \quad (4)$$

$$\frac{d\alpha}{dt} = A'(\alpha) \exp\left[-\frac{E_a(\alpha)}{RT(t)}\right] \quad (5)$$

$$t_a = \int_0^t dt = \int_0^\alpha \frac{d\alpha}{\alpha_0 A'(\alpha) \exp\left[-\frac{E_a(\alpha)}{RT(t)}\right]} \quad (6)$$

$$\ln\left(\frac{d\alpha}{dt}\right) = \ln(A'(\alpha)) - \frac{E_a(\alpha)}{RT(t)} \quad (7)$$

where A is the frequency factor, $f(\alpha)$ is the reaction model, t is the reaction time, and T is the temperature.

Thermal activity monitor III

Isothermal calorimetry, TAM III, was used to explore the changes in the material's thermal response under constant temperature; TAM III involves a continuous and highly thermally sensitive thermostat system and equipment for detecting the stability of the material. The liquid in the thermostat of TAM III was mineral oil, contained in a reactor with a total volume of 25.0 L. Because an external heating thermostat was used and the bottom of the micro-heater controlled the mineral oil temperature, a perfect isothermal effect was achieved. The temperatures used were 15.0–150.0 °C, and the maximum change in temperature over one day was less than 0.0001 °C. The decomposition of the sample was thus measured using

TAM III under isothermal conditions [6]. TAM III Assistant™ software was further used to govern the thermostat and calculate thermokinetic parameters, which were then used to validate the simulation results of the differential isoconversional kinetic analysis.

TAM III was used to determine the thermal decomposition reactions of 88.0 mass% TMCH and 88.0 mass% TMCH mixed with either 5.0 mass% CuCl_2 or FeCl_3 . The mass of the sample used in a cell was 100.0 mg of TMCH mixed with 10.0 mg of CuCl_2 or FeCl_3 at 60.0, 70.0, 80.0, or 90.0 °C. TMR was used as a safety index to evaluate the degree of hazard; therefore, we used TMR_{iso} to evaluate the runaway hazard of TMCH [30].

Results and discussion

Thermal analysis of DSC tests

The oxygen balance (OB %) indicates whether a reactant molecule contains a surplus or insufficient amount of oxygen available for oxidation during combustion. The OB % of TMCH was -248.6 , indicating low thermal hazard. The DSC results were measured by using a PerkinElmer DSC8500 with thermal analysis, determining the heat of decomposition and T_0 under different temperatures. The thermal characteristics of pure TMCH and TMCH mixed with 5.0 mass% CuCl_2 or FeCl_3 are presented in Tables 1–4. The average ΔH_d values of pure TMCH, TMCH mixed with CuCl_2 , and TMCH mixed with FeCl_3 were 1584.8, 898.9, and 1161.1 J g^{-1} , respectively. ΔH_d was not changed in any systematic way when M and β were altered in the pure TMCH DSC experiments. The highest ΔH_d value was 1890.9 J g^{-1} , obtained when β was 8.0 °C min^{-1} and M was only 0.4 mg.

For mixed TMCH and CuCl_2 , ΔH_d was also neither constant, nor did it change systematically. The ΔH_d value at $\beta = 0.5$ °C min^{-1} was 1369.2 J g^{-1} , but the ΔH_d values at different β values in this set of experiments were scattered between 709.8 and 814.4 J g^{-1} . For TMCH mixed with FeCl_3 , the calculated ΔH_d values were distributed between 862.9 and 1374.7 J g^{-1} , comparatively higher than the values for TMCH mixed with CuCl_2 . Compared with that of pure TMCH, the ΔH_d value of TMCH mixed with CuCl_2 or FeCl_3 was lower and the T_0 value of TMCH mixed with CuCl_2 or FeCl_3 was lower. Only one exothermic peak was detected during the DSC tests of TMCH.

Figure 2 illustrates the DSC curves of pure TMCH when different heating rates were used. There is a consistent trend in the curves, with the height of the curve's peak dramatically increased at high β . Because of the excellent consistency observed in the DSC experiments, the E_a value of pure TMCH was calculated with a high degree of

Table 1 Hazard of TMCH mixed of CuCl₂ or FeCl₃ as assessed using React95 [31]

Substances	Hazard analysis
TMCH mixed with CuCl ₂	<ol style="list-style-type: none"> 1. Heat generated from chemical reaction may initiate explosion 2. Heat generation by chemical reaction may cause pressurization 3. Contact with substance liberates toxic gas causes pressurization
TMCH mixed with FeCl ₃	<ol style="list-style-type: none"> 1. Heat generated from chemical reaction may initiate explosion 2. Heat generation by chemical reaction may cause pressurization 3. Contact with substance liberates toxic gas causes pressurization

Table 2 Calorimetric data from DSC tests of TMCH 88.0 mass%

Sample	<i>m</i> /mg	β /°C min ⁻¹	<i>T</i> ₀ /°C	<i>T</i> _{max} /°C	ΔH_d /kJ mol ⁻¹
TMCH 88.0 mass%	2.5	0.5	120.2	123.3	1483.4
	2.0	1.0	121.2	132.1	1395.9
	1.5	2.0	129.8	134.2	1681.6
	0.9	4.0	121.9	145.8	1472.2
	0.4	8.0	123.6	152.9	1890.9

Table 3 Calorimetric data from DSC tests of TMCH 88.0 mass% mixed with 5.0 mass% CuCl₂

Samples	<i>m</i> /mg	β /°C min ⁻¹	<i>T</i> ₀ /°C	<i>T</i> _{max} /°C	ΔH_d /kJ mol ⁻¹
TMCH 88.0 mass% + 5.0 mass% CuCl ₂	6.9	0.5	113.0	119.4	1369.2
	6.1	1.0	108.6	125.9	779.9
	4.9	2.0	113.5	133.6	761.2
	4.1	4.0	122.3	140.7	874.4
	2.9	8.0	129.2	149.5	709.8

confidence. The DSC curves of TMCH mixed with CuCl₂ or FeCl₃ also illustrate one dominating exothermic peak, and the *T*₀ value of TMCH mixed with CuCl₂ or FeCl₃ was between 108.6 and 137.1 °C (Figs. 2–4). The results from various heating rates indicated that the faster the reaction was, the greater the intensity of heat omitted became, whereas the lower the heating rate was, the later the appearance of the exothermic peak became.

Figure 5 illustrates a plot of the natural logarithm of the heating rate versus the reciprocal of the absolute temperature for TMCH and the TMCH mixtures. Through the application of the Kissinger kinetic equation, the *E*_a values

of TMCH, TMCH mixed with CuCl₂, and TMCH mixed with FeCl₂ were determined to be 129.8, 127.1, and 143.1 kJ mol⁻¹, respectively. The *E*_a value was lowest for TMCH mixed with CuCl₂, whereas the *E*_a value of TMCH mixed with FeCl₂ was substantially higher than those of the other two samples.

Thermal simulation using isoconversional kinetic analysis

DSC can acquire the experimental parameters of pure TMCH or TMCH mixed with 5.0 mass% CuCl₂ or FeCl₃,

Table 4 Calorimetric data from DSC tests of TMCH 88.0 mass% mixed with 5.0 mass% FeCl₃

Samples	<i>m</i> /mg	β /°C min ⁻¹	<i>T</i> ₀ /°C	<i>T</i> _{max} /°C	ΔH_d /kJ mol ⁻¹
TMCH 88.0 mass% + 5.0 mass% FeCl ₃	7.3	0.5	109.1	124.5	1027.4
	5.8	1.0	109.7	130.3	1294.2
	4.9	2.0	137.1	137.8	1374.7
	3.9	4.0	124.9	144.2	862.9
	3.0	8.0	127.6	151.3	1246.3

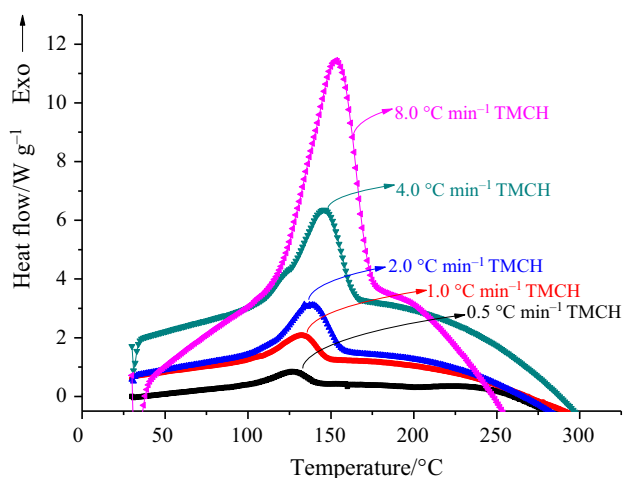


Fig. 2 DSC curves of heat flow versus temperature for pure TMCH decomposition at heating rates of 0.5, 1.0, 2.0, 4.0, and 8.0 °C min⁻¹

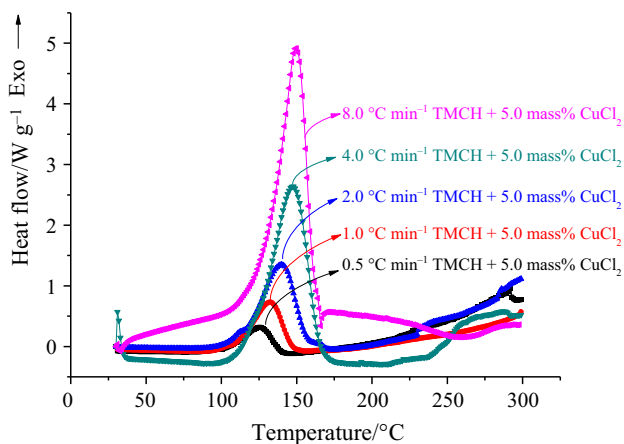


Fig. 3 DSC curves of heat flow versus temperature for the decomposition of TMCH mixed with 5.0 mass% CuCl₂ at heating rates of 0.5, 1.0, 2.0, 4.0, and 8.0 °C min⁻¹

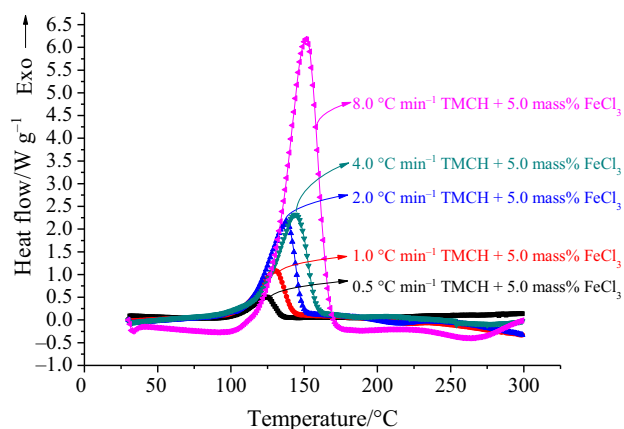


Fig. 4 DSC curves of heat flow versus temperature for the decomposition of TMCH mixed with 5.0 mass% FeCl₃ at heating rates of 0.5, 1.0, 2.0, 4.0, and 8.0 °C min⁻¹

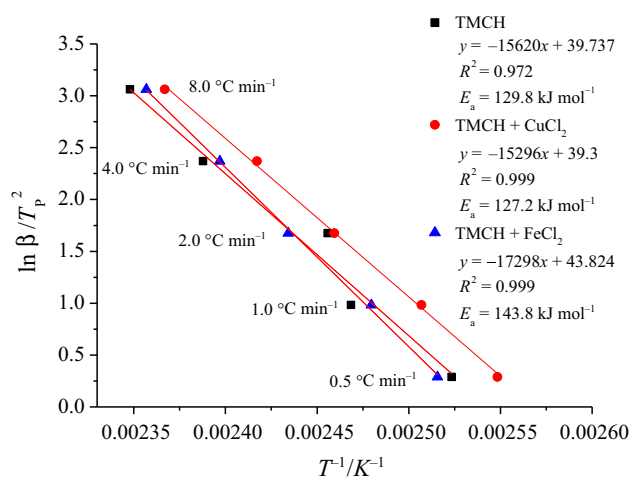


Fig. 5 E_a analysis graphs for TMCH, TMCH mixed with CuCl₂, and FeCl₂ at heating rates of 0.5, 1.0, 2.0, 4.0, and 8.0 °C min⁻¹ using the Kissinger kinetic equation

such as the sample mass, reaction time, reaction temperature, and heat flow; such parameters can be used to execute isoconversional kinetic analysis. The relationship between heating rate and E_a was determined through isoconversional kinetic analysis. Using isoconversional kinetic analysis, E_a of pure TMCH, TMCH mixed with CuCl₂, and TMCH mixed with FeCl₃ were obtained from a linear regression model for the natural logarithm of the heating rate versus the reciprocal of absolute temperature. The corresponding temperatures were obtained from the peak of heat flow of five different heating rates. According to the plots in Fig. 6, the E_a values calculated using non-isothermal heating rates for pure TMCH, TMCH mixed with CuCl₂, and TMCH mixed with FeCl₃ were 137.9, 119.5, and 132.6 kJ mol⁻¹, respectively. The linear regression model had an excellent fit, and Fig. 6 shows the high accuracy of the thermokinetic model of the three

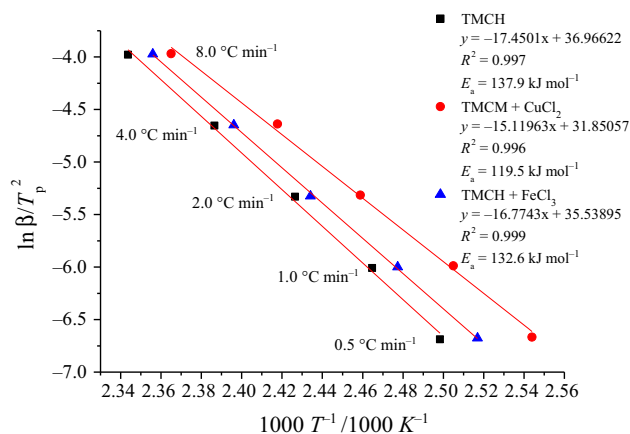


Fig. 6 E_a analysis graph of TMCH, TMCH mixed with CuCl₂, and TMCH mixed with FeCl₃ determined from isoconversional kinetic analysis with different nonisothermal heating rates of 0.5, 1.0, 2.0, 4.0, and 8.0 °C min⁻¹

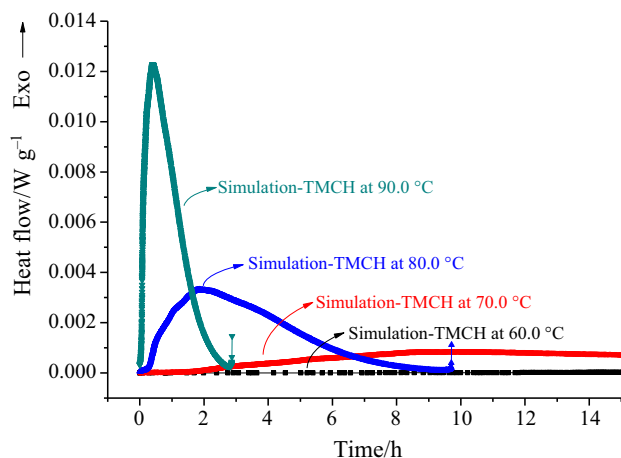


Fig. 7 Differential isoconversional kinetic analysis simulation of isothermal curves for decomposition of pure TMCH at 60.0, 70.0, 80.0, and 90.0 °C

TMCH mixtures for varying heating rate. The E_a value was substantially lower for TMCH mixed with CuCl_2 than for the other two samples.

The results of E_a analysis for TMCH and TMCH mixed with different metal ions are similar because they were calculated using the Kissinger kinetic equation. Of the three samples subjected to isoconversional kinetic analysis, TMCH mixed with CuCl_2 exhibited the lowest E_a value. Therefore, isoconversional kinetic analysis effectively simulated the exothermic reactions in pure TMCH, TMCH mixed with 5.0 mass% CuCl_2 , and TMCH mixed with 5.0 mass% FeCl_3 under isothermal conditions (i.e., temperatures of 60.0, 70.0, 80.0, and 90.0 °C), and Figs. 7–9 display the corresponding curves of heat flow versus time for these samples, respectively. These figures indicate that for TMCH mixed with 5.0 mass% CuCl_2 or 5.0 mass% FeCl_3 , the isothermal temperature was higher, the heat flow was enhanced, and the reaction was prematurely

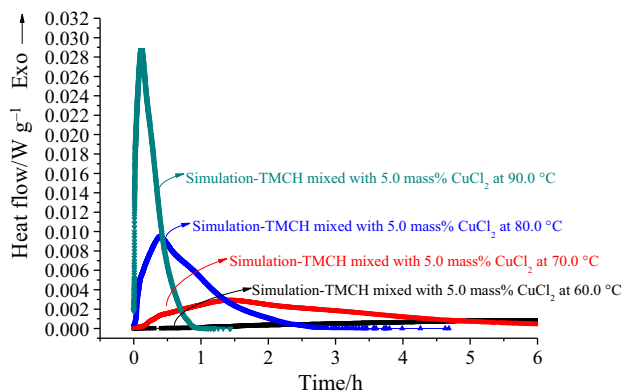


Fig. 8 Differential isoconversional kinetic analysis simulation of isothermal curves for decomposition of TMCH mixed with 5.0 mass% CuCl_2 at 60.0, 70.0, 80.0, and 90.0 °C

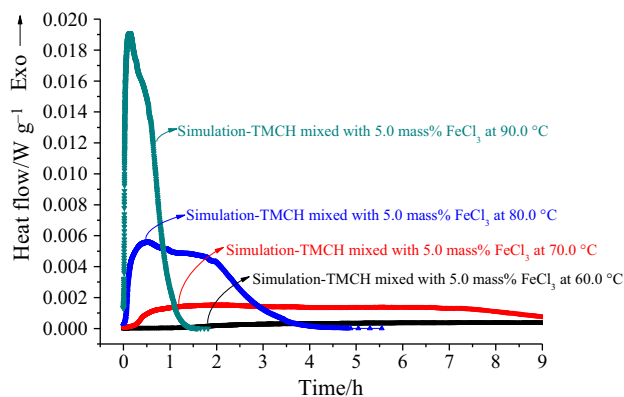


Fig. 9 Differential isoconversional kinetic analysis simulation of isothermal curves for decomposition of TMCH mixed with 5.0 mass% FeCl_3 at 60.0, 70.0, 80.0, and 90.0 °C

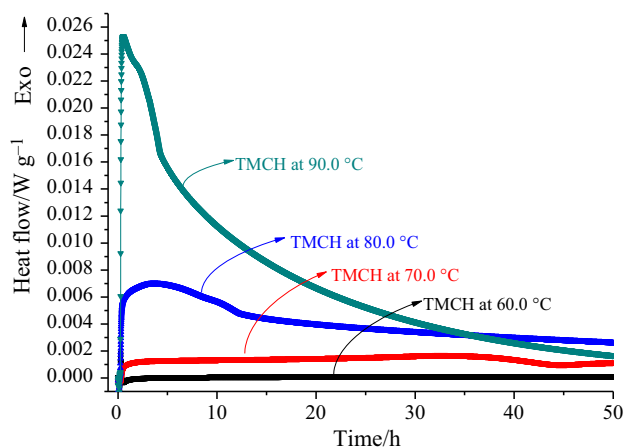


Fig. 10 TAM III thermal curves of heat flow versus time for decomposition of pure TMCH at 60.0, 70.0, 80.0, and 90.0 °C

terminated; the maximum reaction time simulated was 15 h. The isothermal simulation results (Figs. 7–9) were effectively exhibited but not fitting perfectly. It is because the isothermal simulation data were calculated from non-isothermal conditions by DSC in which the sample mass was poured in 10.0 mg. However, the isothermal experiments (Figs. 10–12) were carried out by TAM III in which the sample mass was high to 100.0 mg.

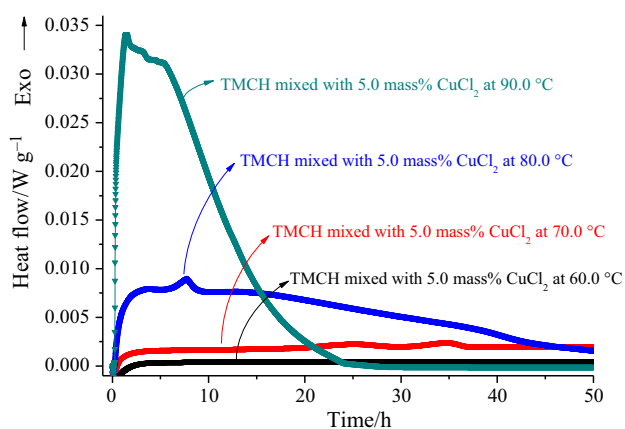
Few exothermic reactions occurred in any sample when the temperature was 60.0 °C; however, small exothermic reactions occurred after 2 h at 70.0 °C. At 80.0 °C, nevertheless, substantial exothermic phenomena occurred in the TMCH and TMCH mixtures during the isothermal simulations. The heat flow was not large but was sufficient to cause heat accumulation if a storage container contained a large amount of chemicals. At 90.0 °C, the maximum heat flow was significantly higher and TMR_{iso} was shorter than those at lower temperatures. The simulation results

Table 5 Scanning data of the thermal runaway decomposition of pure TMCH and TMCH mixed with metal ions at 60.0 °C using TAM III

Samples	<i>m</i> /mg	<i>TMR</i> _{iso} /h	Highest heat flow/W g ⁻¹	ΔH_d /J g ⁻¹
TMCH 88.0 mass%	101.9	189.3	0.00018	0.054
TMCH 88.0 mass% + 5.0 mass% CuCl ₂	110.7	106.4	0.00046	12.529
TMCH 88.0 mass% + 5.0 mass% FeCl ₃	110.9	131.7	0.00038	20.157

Table 6 Scanning data of the thermal runaway decomposition of pure TMCH and TMCH mixed with metal ions at 70.0 °C using TAM III

Samples	<i>m</i> /mg	<i>TMR</i> _{iso} /h	Highest heat flow/W g ⁻¹	ΔH_d /J g ⁻¹
TMCH 88.0 mass%	102.8	32.34	0.00163	14.540
TMCH 88.0 mass% + 5.0 mass% CuCl ₂	109.6	25.34	0.00223	26.849
TMCH 88.0 mass% + 5.0 mass% FeCl ₃	110.9	19.74	0.00188	21.845

**Fig. 11** TAM III thermal curves of heat flow versus time for decomposition of TMCH mixed with 5 mass% CuCl₂ at 60, 70, 80, and 90 °C

thus reveal that the maximum heat flow of TMCH mixed with metal ions was remarkably higher than that of pure TMCH. This phenomenon was more noticeable when the isothermal surroundings were at a higher temperature.

Isothermal analysis of TAM III tests

The results of heat flow versus time for pure TMCH or TMCH mixed with 5.0 mass% metal ions at different isothermal temperatures determined using TAM III are presented in Figs. 10–12. The terminal reaction time decreased as the experimental temperature was increased. *TMR*_{iso} decreased when the isothermal temperature was increased, down from 189.3 to 0.5 h for pure TMCH when the isothermal temperature was changed from 60.0 to 90.0 °C, as detailed in Tables 5–8. *TMR*_{iso} since TMCH mixed with CuCl₂ was dramatically reduced from 106.4 to 1.5 h, although the heat flow in the sample was greater than that in pure TMCH or TMCH mixed with FeCl₃, as demonstrated in Figs. 10–12. At 90.0 °C, the heat flow in TMCH mixed with CuCl₂ was more unstable than that in pure TMCH or TMCH mixed with FeCl₃. *TMR*_{iso} of pure TMCH was shorter than that of TMCH mixed with CuCl₂ at isothermal temperatures of 60.0, 70.0, 80.0, and 90.0 °C. However, the *TMR*_{iso} duration observed for pure TMCH in the TAM III isothermal experiment was shorter than those

Table 7 Scanning data of the thermal runaway decomposition of pure TMCH and TMCH mixed with metal ions at 80.0 °C using TAM III

Samples	<i>m</i> /mg	<i>TMR</i> _{iso} /h	Highest heat flow/W g ⁻¹	ΔH_d /J g ⁻¹
TMCH 88.0 mass%	101.9	3.5	0.00695	23.102
TMCH 88.0 mass% + 5.0 mass% CuCl ₂	110.0	7.7	0.00889	85.263
TMCH 88.0 mass% + 5.0 mass% FeCl ₃	109.6	13.9	0.00506	29.619

Table 8 Scanning data of the thermal runaway decomposition of pure TMCH and TMCH mixed with metal ions at 90.0 °C using TAM III

Samples	<i>m</i> /mg	<i>TMR</i> _{iso} /h	Highest heat flow/W g ⁻¹	ΔH_d /J g ⁻¹
TMCH 88.0 mass%	101.1	0.5	0.02531	–
TMCH 88.0 mass% + 5.0 mass% CuCl ₂	110.8	1.5	0.03410	146.29
TMCH 88.0 mass% + 5.0 mass% FeCl ₃	111.0	2.3	0.02823	100.02

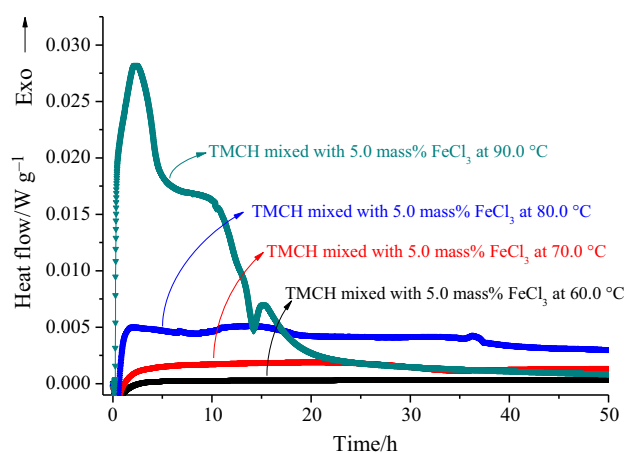


Fig. 12 TAM III thermal curves of heat flow versus time for decomposition of TMCH mixed with 5.0 mass% FeCl_3 at 60.0, 70.0, 80.0, and 90.0 °C

observed in the other isothermal experiments at 80.0 and 90.0 °C.

When TMCH was mixed with FeCl_3 , TMR_{iso} decreased remarkably from 131.7 to 2.3 h when the temperature was increased from 60.0 to 90.0 °C. Although these TMR_{iso} durations were shorter than those for pure TMCH, the heat flow was still substantial. As illustrated in Figs. 11 and 12, the TMR_{iso} duration of TMCH mixed with CuCl_2 was shorter because the exothermic peak in the corresponding thermal curve was significantly sharper and higher than that in the curve for TMCH mixed with FeCl_3 . Both differential isoconversional kinetic analysis simulations and TAM III isothermal experiments indicated that the heat flow of TMCH mixed with CuCl_2 was prominently higher when a higher temperature was used. The reaction time determined in the TAM III experiment was much longer than that calculated through differential isoconversional kinetic analysis simulations. However, the reactivity levels of TMCH mixed with FeCl_3 demonstrated using simulations and experiments were similar, as illustrated by the exothermic peaks.

In summary, results from experiments and simulations under isothermal conditions matched reasonably well. Greater heat flow was discovered at higher temperatures, with TMR_{iso} correspondingly shorter.

Conclusions

Although no obvious catalysis was observed in TMCH mixed with metal ions, the effect of high heat flow at high temperatures should not be ignored. DSC revealed that T_0 was decreased as the heating rate was increased when TMCH was mixed with CuCl_2 or FeCl_3 , and that heat flow

was reduced for TMCH mixed with CuCl_2 in the non-isothermal tests compared with pure TMCH. The results differed when isothermal temperatures were used in experiments. TMCH mixed with metal ions accumulates heat and thus produces thermal energy. TMR_{iso} was shortened at isothermal temperatures when CuCl_2 or FeCl_3 was added to TMCH. The E_a value of pure TMCH was lower than that of TMCH mixed with FeCl_3 , indicating that reactions could occur readily in pure TMCH.

In addition to OP storage and transportation challenges, the chemical industry must handle waste stream treatments wherein mixtures are not completely recycled. This may result in incompatible reactions, leading to a thermal accident. In the future, OPs mixed with metal ions must be investigated using schematic and systematically approaches with analytical assessments as well as the identification of reaction mechanisms.

Acknowledgements The authors thank Ms. Vaefun Shi and Mr. Ao Chen for their assistance in solving the problems presented by differential isoconversional kinetic analysis simulations. Financial support for this study was graciously provided by the External Cooperation Program of Chinese Academy of Sciences, Grant No.: GJHZ1726.

References

- Chen WC, Shu CM. Prediction of thermal hazard for TBPTMH mixed with BPO through DSC and isoconversional kinetics analysis. *J Therm Anal Calorim.* 2016;126:1937–45.
- Chi JH, Wu SH, Shu CM. Thermal explosion analysis of methyl ethyl ketone peroxide by non-isothermal and isothermal calorimetric applications. *J Hazard Mater.* 2009;171:1145–9.
- Duh YS, Xu XH, Kao CS. Hazard ratings for organic peroxides. *Process Saf Prog.* 2008;27:89–99.
- Li AC, Tsai YT, Wu SH, Chiu CW, Shen SJ, Cheng RH, Shu CM. Thermal runaway analysis for two organic peroxides with H_2O and dry fire-extinguishing chemicals by DSC and VSP2. *J Therm Anal Calorim.* 2013;113:1611–8.
- Lin YF, Lin CP, Chen LY, Su TS, Tseng JM. Effect of different concentrations of acetone for the decomposition reactions of peroxyketal peroxides. *Thermochim Acta.* 2012;527:27–32.
- Liu SH, Hou HY, Shu CM. Effects of thermal runaway hazard for three organic peroxides conducted by acids and alkalines with DSC, VSP2, and TAM III. *Thermochim Acta.* 2013;556:226–32.
- Wang TS, Liu SH, Qian XM, Shu CM. Isothermal hazards evaluation of benzoyl peroxide mixed with benzoic acid via TAM III test. *J Therm Anal Calorim.* 2013;113:1625–31.
- Weng SY, Liu SH, Tsai LC, Hsieh TF, Ma CM, Shu CM. Thermokinetics simulation for multi-walled carbon nanotubes with sodium alginate by advanced kinetics and technology solutions. *J Therm Anal Calorim.* 2013;113:1603–10.
- Lin WH, Wu SH, Shiu GY, Shieh SS, Shu CM. Self-accelerating decomposition temperature (SADT) calculation of methyl ethyl ketone peroxide using an adiabatic calorimeter and model. *J Therm Anal Calorim.* 2009;95:645–51.
- Chen CJ, Chi JH, Wu SH, Chen CT, Tsai HF. Fundamental thermal hazard investigation for *tert*-butyl peroxide reactor using DSC and TGA techniques. *J Appl Fire Sci.* 2012;21:53–63.

- Chu YC, Tsai FC, Lin FR, Chiang TC, Shu CM. Evaluation unexpected energy released for three liquid organic peroxides. *Energy Educ Sci Tech Pt A*. 2013;30:977–82.
- Jhu CY, Wang YW, Wen CY, Shu CM. Thermal runaway potential of LiCoO₂ and Li (Ni_{1/3}Co_{1/3}Mn_{1/3}) O₂ batteries determined with adiabatic calorimetry methodology. *Appl Energy*. 2012;100:127–31.
- Lu TY, Chen JL, Chi JH, Wu SH, Jian HL. Thermal explosion analysis of *tert*-butyl peroxide by calorimetric technology and mathematical model development. *J Appl Fire Sci*. 2012;21:85–97.
- Ma H, Yan B, Li Z, Guan Y, Song J, Xu K, Hu R. Preparation non-isothermal decomposition kinetics, heat capacity and adiabatic time-to-explosion of NTO· DNAZ. *J Hazard Mater*. 2009;169:1068–73.
- Tsai YT, You ML, Qian XM, Shu CM. Calorimetric techniques combined with various thermokinetic models to evaluate incompatible hazard of *tert*-butyl peroxy-2-ethyl hexanoate mixed with metal ions. *Ind Eng Chem Res*. 2013;52:8206–15.
- Zang N, Qian XM, Liao JY, Shu CM. Thermal stability of lauroyl peroxide by isoconversional kinetics evaluation and finite element analysis. *J Taiwan Inst Chem Eng*. 2014;45:461–7.
- Kumasaki M. An explosion of a tank car carrying waste hydrogen peroxide. *J Loss Prev Process Ind*. 2006;19:307–11.
- Liu SH, Lin CP, Shu CM. Thermokinetic parameters and thermal hazard evaluation for three organic peroxides by DSC and TAM III. *J Therm Anal Calorim*. 2011;106:165–72.
- Deng J, Zhao J-Y, Huang A-C, Zhang Y-N, Wang C-P, Shu C-M. Thermal behavior and microcharacterization analysis of second-oxidized coal. *J Therm Anal Calorim*. 2017;127:439–48.
- Chen KY, Wu SH, Wang YW, Shu CM. Runaway reaction and thermal hazards simulation of cumene hydroperoxide by DSC. *J Loss Prev Process Ind*. 2008;21:101–9.
- Safety and handling of organic peroxides. A guide, organic peroxide producers safety division. Washington, DC: The Society of the Plastics Industry (SPI) Inc; 1999.
- Wu LK, Chen KY, Cheng SY, Lee BS, Shu CM. Thermal decomposition of hydrogen peroxide in the presence of sulfuric acid. *J Therm Anal Calorim*. 2008;93:115–20.
- Center for Chemical Process Safety. Guidelines for chemical reactivity evaluation and application to process design. New York: AIChE; 1995.
- Frurip DJ. Using the ASTM CHETAH program in chemical process hazard evaluation. *Process Saf Prog*. 1992;11:224–8.
- Lothrop WC, Handrick GR. The relationship between performance and constitution of pure organic explosive compounds. *Chem Rev*. 1948;44:419–45.
- Stanley ES, Melhem GA. A review of ASTM CHETAH 7.0 hazard evaluation criteria. *J Loss Prev Process Ind*. 1995;8:261–4.
- de Godois Baroni É, Tannous K, Rueda-Ordóñez YJ, Tinoco-Navarro LK. The applicability of isoconversional models in estimating the kinetic parameters of biomass pyrolysis. *J Therm Anal Calorim*. 2016;123:909–17.
- Matos J, Oliveira JF, Magalhães D, Dubaj T, Cibulková Z, Šimon P. Kinetics of ambuphylline decomposition studied by the incremental isoconversional method. *J Therm Anal Calorim*. 2016;123:1031–6.
- Pérez A, Lopez-Olmedo JP, Farjas J, Roura P. Isoconversional analysis of copper recrystallization. *J Therm Anal Calorim*. 2016;25:667–72.
- Tseng JM, Liu MY, Chen SL, Hwang WT, Gupta JP, Shu CM. Runaway effects of nitric acid on methyl ethyl ketone peroxide by TAM III tests. *J Therm Anal Calorim*. 2009;96:789–93.
- Chemical reactivity worksheet. Office of response and restoration. New Castle, DE: NOAA; 2016.